

The 2MASS galaxy angular power spectrum: Probing the galaxy distribution to Gigaparsec scales

W.J. Frith^{*}, P.J. Outram & T. Shanks

Dept. of Physics, Univ. of Durham, South Road, Durham DH1 3LE, UK

Accepted 2005. Received 2005; in original form 2005

ABSTRACT

We present an angular power spectrum analysis of the 2 Micron All Sky Survey (2MASS) full release extended source catalogue. The main sample used includes 518 576 galaxies below an extinction-corrected magnitude of $K_s=13.5$ and limited to $|b| > 20^\circ$. The power spectrum results provide an estimate of the galaxy density fluctuations at extremely large scales, $r \lesssim 1000 h^{-1}$ Mpc. We compare this with mock predictions constructed from the Λ CDM Hubble Volume mock catalogue. We find that over the range $1 \leq l \leq 100$ the 2MASS C_l is steeper than that for the Hubble Volume model. However, in the linear regime ($l \leq 30$) there is good agreement between the two. We investigate in detail the effects of possible sources of systematic error. Converting linear power spectrum predictions for the form of the three-dimensional matter power spectrum, $P(k)$, and assuming a flat CDM cosmology, a primordial $n_s=1$ spectrum and negligible neutrino mass, we perform fits to the galaxy angular power spectrum at large linear scales ($l \leq 30$, corresponding to $r \gtrsim 50 h^{-1}$ Mpc). We obtain constraints on the galaxy power spectrum shape of $\Gamma_{eff} = 0.14 \pm 0.02$, in good agreement with previous estimates inferred at smaller scales. We also constrain the galaxy power spectrum normalisation to $(\sigma_8 b_K)^2 = 1.36 \pm 0.10$; in combination with previous constraints on σ_8 we infer a K_s -band bias of $b_K = 1.39 \pm 0.12$. We are also able to provide weak constraints on $\Omega_m h$ and Ω_b/Ω_m . These results are based on the usual assumption that the errors derived from the Hubble Volume mocks are applicable to all other models. If we instead assume that the error is proportional to the C_l amplitude then the constraints weaken; for example it becomes more difficult to reject cosmologies with lower Γ_{eff} .

Key words: cosmological parameters - cosmology: observations - large-scale structure of the Universe - infrared: galaxies

1 INTRODUCTION

The nature of galaxy fluctuations at extremely large scales ($r \lesssim 1000 h^{-1}$ Mpc) is poorly constrained. Over the last decade, large galaxy surveys have constrained the form of the galaxy density field to a few hundred Megaparsecs. However, the agreement with the concordance model at these scales can only be weakly inferred. Indeed, recent evidence has suggested that there may be excess power over the expected Λ CDM form to the three-dimensional power spectrum of matter, $P(k)$, at large scales (Frith et al. 2005, 2004, 2003; Buswell et al. 2004) arising from large inhomogeneities in the local galaxy distribution.

In recent years, large redshift surveys of both galaxies (Cole et al. 2005; Percival et al. 2001; Zehavi et al. 2002) and QSOs (Outram et al. 2003) have determined $P(k)$ at relatively small scales. Using the 2dF Galaxy

Redshift Survey (2dFGRS), Cole et al. (2005) have constrained the form of galaxy density fluctuations to scales of $r \approx 300 h^{-1}$ Mpc and the associated cosmological parameters to $\Omega_m h = 0.168 \pm 0.016$ and $\Omega_b/\Omega_m = 0.185 \pm 0.046$ (assuming $h=0.72$). However, determining the power spectrum through such redshift surveys suffers from large statistical uncertainty at large scales due to the relatively few objects available, as well as uncertainties arising from cosmic variance due to the relatively small volumes surveyed.

Using imaging surveys as opposed to redshift surveys provides a greater number of objects over larger solid angles. With angular power spectrum analysis of such surveys it is therefore possible to constrain the form of galaxy fluctuations to extremely large scales. However, since the clustering signal from a particular scale in real space is smeared over a range of angular scales, cosmological constraints through comparisons with linear theory predictions at smaller scales cannot be made; the departure from linearity at scales of $r \lesssim 40 h^{-1}$ Mpc (Percival et al. 2001) affects the clustering

^{*} E-mail: w.j.frith@durham.ac.uk

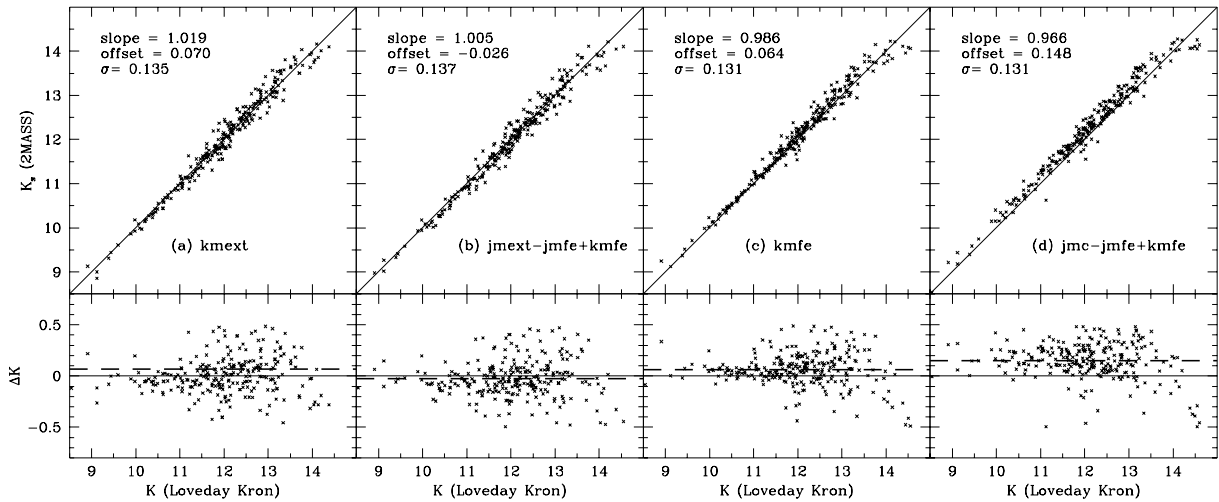


Figure 1. A selection of K_s -band magnitude estimates from the 2MASS full release compared with Loveday (2000) K -band photometry. In each case the lower panels display the residual. The $x = y$ slope is indicated by a solid line, while the mean offset is indicated in the lower panel by a dashed line. This offset (in magnitudes), the best fit slope determined from least squares fits and the rms scatter are indicated for each magnitude estimate. We estimate the magnitudes directly from the (a) K_s -band extrapolated and (c) K_s -band fiducial elliptical Kron magnitudes, and also from the (b) J -band extrapolated and (d) J -band circular Kron magnitudes colour-corrected to the K_s -band using the J and K_s -band fiducial elliptical Kron magnitudes.

signal in the angular power spectrum over a wide range of scales. Nevertheless at large scales, where this effect is insignificant, angular power spectrum analysis represents one of the most effective probes of local large-scale structure.

Previously, the galaxy angular power spectrum has been determined for the Sloan Digital Sky Survey Early Data Release, the Edinburgh-Durham Southern Galaxy Catalogue, and a sample of IRAS galaxies (Tegmark et al. 2002; Huterer, Knox & Nichol 2001; Scharf et al. 1992, respectively), which along with the recent analyses of redshift surveys has constrained the form of galaxy fluctuations to $r \approx 300 h^{-1}$ Mpc.

The 2 Micron All Sky Survey (2MASS) has recently been completed and provides K_s , H and J -band photometry for $\approx 1.6 \times 10^6$ extended sources over the entire sky to $K_s \gtrsim 13.5$ (Jarrett 2004; Jarrett et al. 2000); at the time of writing this dataset represents the largest all sky galaxy survey. The 2MASS data therefore represents a uniquely powerful probe of the local galaxy density field at large scales; applying a galactic latitude cut of $|b| > 20^\circ$ in order to remove regions of high extinction and stellar contamination yields a sample containing 518 576 $K_s < 13.5$ galaxies, probing a volume approximately 5 times larger than the final 2dF Galaxy Redshift Survey (2dFGRS) volume. A further advantage of 2MASS over previous datasets is that the photometry is extremely accurate with high completeness; the photometric zero-point calibration is accurate to 2-3 per cent; galaxy

identification is ≈ 99 per cent reliable and the galaxy catalogue is >90 per cent complete for $|b| > 20^\circ$ (Jarrett 2004).

In this paper, we use data from the 2MASS final release extended source catalogue to determine the K_s -band galaxy angular power spectrum with the aim of determining the form of the clustering of galaxies at extremely large scales, and constraining the shape and normalisation of the power spectrum. In section 2, we describe the 2MASS dataset and the magnitude estimator used. The method of analysis is outlined and the 2MASS angular power spectrum is determined and compared to mock power spectra in section 3. In section 4, we investigate various sources of systematic error. We determine constraints for various cosmological parameters in section 5. The conclusions follow in section 6.

2 DATA

2.1 The 2MASS Extended Source Catalogue

The 2 Micron All Sky Survey (2MASS) final release extended source catalogue provides K_s , H and J -band photometry for over 1.6×10^6 extended sources over the entire sky with high completeness to $K_s = 13.5$ (Jarrett 2004).

Previously, in order to estimate the total K_s -band magnitudes from the 2MASS second incremental release data, Cole et al. (2001) used the deeper J -band Kron magnitudes, colour-corrected to the K_s -band via the J and K_s default

aperture magnitudes. The accuracy of this magnitude estimator was determined through a comparison with the K -band photometry of Loveday (2000); the Loveday photometry had better signal-to-noise and resolution than the 2MASS scans and so enabled more accurate 2MASS magnitudes to be determined.

The final release data uses revised magnitude estimates and the default aperture magnitudes used in Cole et al. (2001) have been abandoned (Jarrett - priv. comm.). In Fig. 1 we show a selection of 2MASS K_s -band magnitude estimates with the revised 2MASS photometry compared with the Loveday (2000) photometry used previously. In the place of the default aperture magnitudes used in Cole et al. (2001), we use fiducial elliptical Kron magnitudes in panels (b) and (d) to colour-correct the J -band magnitudes to the K_s -band. Of the many different magnitude estimates examined, the most accurate in terms of the scale error between the Loveday and 2MASS photometry and the zero-point offset uses the J -band extrapolated magnitude colour-corrected to the K_s -band as described above. Using the dust maps of Schlegel et al. (1998), the main galaxy sample uses extinction-corrected K_s -band magnitudes calculated in this way.

In order to verify the usefulness of the magnitude estimator used in this work as an estimate of the total K_s -band magnitude, we perform an internal check via a comparison with the magnitude estimates used in the 2MASS-selected 6dF Galaxy Survey (6dFGS). The 6dFGS K_s -band magnitudes are determined using a surface brightness correction to the K_s -band 20 mag. arcsec⁻² isophotal elliptical aperture magnitude (Jones et al. 2004). We find excellent agreement with a slope of 1.022, an offset of 0.018 magnitudes and a spread of $\sigma=0.048$ magnitudes for $|b| > 20^\circ$ galaxies matched below $K_s = 13.5$.

The 2MASS dataset removes or flags sources identified as artefacts such as diffraction spikes and meteor streaks (Jarrett et al. 2000); we use the 2MASS *cc_flag* to remove such objects. We also employ a colour cut ($J - K_s < 0.7$ and $J - K_s > 1.4$) below $K_s=12$ in order to remove a small number of objects identified as non-extragalactic extended sources (Maller et al. 2003, 2005). In this work, our main sample includes 518 576 $K_s < 13.5$ galaxies above a galactic latitude of $|b| = 20^\circ$. For reference, the surface density is 19.1 deg⁻². We also use a shallower sample limited at $K_s=12.5$ and $|b| > 20^\circ$ which includes 124 264 galaxies and for which the surface density is 4.58 deg⁻².

2.2 The Λ CDM Hubble Volume Simulation

The Hubble Volume catalogues represent the largest volume N -body simulations of the Universe to date. The Λ CDM simulation follows the evolution of 10^9 dark matter particles from $z \approx 50$ over a volume of $3000^3 h^{-3} \text{Mpc}^3$ to a resolution of $\approx 3 h^{-1} \text{Mpc}$. The associated cosmological parameters are $\Omega_m=0.3$, $\Omega_b=0.04$, $h=0.7$, $\sigma_8=0.9$ (Jenkins et al. 1998).

In this work, we construct mock 2MASS catalogues from the $z = 0$ Λ CDM Hubble Volume simulation dark matter particles. We divide the total volume into 27 virtually independent spherical volumes of $r = 500 h^{-1} \text{Mpc}$. These are subjected to the 2MASS selection function:

$$n(z) = \frac{3z^2}{2(\bar{z}/1.412)^3} \exp\left(-\left(\frac{1.412z}{\bar{z}}\right)^{3/2}\right) \quad (1)$$

(Baugh & Efstathiou 1993; Maller et al. 2005) where \bar{z} is determined from the 2MASS-2dFGRS matched sample described in Frith et al. (2005); for reference $\bar{z}=0.074$ for $K_s < 13.5$ and $\bar{z}=0.050$ for $K_s < 12.5$. Equation 1 is normalised to match the total number of observed 2MASS galaxies for $|b| > 20^\circ$. Due to the volume of the 27 mock 2MASS catalogues, the selection function is artificially truncated for the $K_s < 13.5$ mocks at $z \approx 0.156$. However, this has a negligible effect on the work in this paper; at this redshift, ≈ 95 per cent of the galaxies are sampled for $K_s < 13.5$.

3 THE 2MASS ANGULAR POWER SPECTRUM

3.1 Estimating the Power Spectrum

Following the usual method (e.g. Peebles 1973; Hauser & Peebles 1973; Peebles & Hauser 1974; Scharf et al. 1992), the angular power is estimated through a spherical harmonic expansion of the surface density of galaxies. The coefficients of this expansion are determined over the observed solid angle Ω_{obs} :

$$a_l^m = \sum_{N_{gal}} Y_l^m(\theta, \phi) - \mathcal{N} \int_{\Omega_{obs}} Y_l^m(\theta, \phi) d\Omega \quad (2)$$

where $\mathcal{N}=N_{gal}/\Omega_{obs}$ is the observed number of galaxies per steradian. The angular power is then determined:

$$Z_l = \frac{1}{2l+1} \sum_m \frac{|a_l^m|^2}{\mathcal{J}_l^m} \quad (3)$$

where,

$$\mathcal{J}_l^m = \int_{\Omega_{obs}} Y_l^m(\theta, \phi) d\Omega \quad (4)$$

The angular power is then normalised, subtracting the expected shot noise contribution:

$$C_l = \frac{Z_l}{\mathcal{N}} - 1 \quad (5)$$

such that $C_l=0$ corresponds to a random distribution.

3.2 Fitting to the Power Spectrum

In order to compare the angular power spectrum with cosmological predictions, we determine an expected form for the angular power spectrum for various cosmological parameters using the relation between the three and two-dimensional power spectra:

$$|a_l^m|^2 = \frac{2}{\pi} \int \left(\int r^2 \Phi(r) j_l(kr) dr \right)^2 k^2 P(k) dk + \mathcal{N} \quad (6)$$

(Scharf et al. 1992; Tegmark et al. 2002; Huterer, Knox & Nichol 2001), which we normalise as before. Here, $\Phi(r)$ is the 2MASS selection function, and j_l is a spherical Bessel function. The 2MASS selection function is determined using equation 1.

We use the transfer function fitting formulae of Eisenstein & Hu (1998) to obtain a linear theory prediction

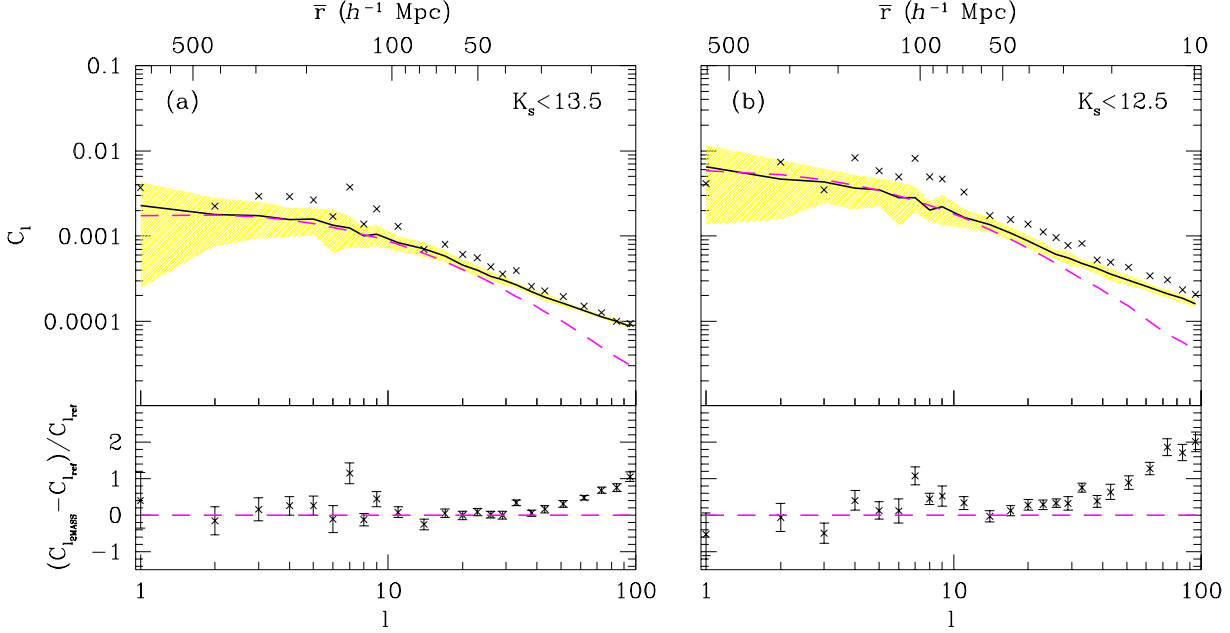


Figure 2. The $|b| > 20^\circ$ 2MASS galaxy angular power spectrum for (a) 518 576 $K_s < 13.5$ and (b) 124 264 $K_s < 12.5$ galaxies. The crosses indicate the 2MASS datapoints with the shaded region and solid line indicating the 1σ spread and mean power spectrum of the 27 mock unbiased 2MASS catalogues constructed from the Λ CDM Hubble Volume mock catalogue as described in section 2.2. In each case, unbiased linear theory models corresponding to the Hubble Volume mock catalogue input parameters of $\Omega_m=0.3$, $\Omega_b=0.04$, $h=0.7$ and $\sigma_8=0.9$ are indicated by the dashed lines. In the lower panels we show the fractional deviation of the 2MASS power spectrum from this model applying the best fit power spectrum normalisation, $\sigma_8 b_k^2=1.36$, (determined in section 5 for the $K_s < 13.5$ sample) to the linear prediction, with errors taken from the mock 2MASS 1σ spread. In addition we indicate the approximate mean distance scale probed by the data for each l -mode on the top x -axis.

for the dark matter power spectrum, $P(k)$, with input parameters for the matter, vacuum, baryon and neutrino densities (Ω_m , Ω_Λ , Ω_b and Ω_ν), h (such that $H_0 = 100h$) and matter power spectrum normalisation (σ_8). We also employ a linear biasing scheme such that $P_{gal}(k)=b^2 P_{matter}(k)$ to provide a linear prediction for the galaxy $P(k)$. This is then transformed to a galaxy angular power spectrum prediction using the spherical Bessel function transform in equation 6.

3.3 Results

The angular power spectrum for 518 576 $K_s < 13.5$, $|b| > 20^\circ$ 2MASS galaxies is presented in Fig. 2a, determined through a spherical harmonic expansion of the galaxy number density as described in section 3.1. In order to determine the expected scatter due to cosmic variance we determine the angular power spectrum for the 27 unbiased mock 2MASS catalogues constructed from the Λ CDM Hubble Volume simulation described in section 2.2; the mean and 1σ spread are indicated by the solid line and shaded region. On the top x -axis we also indicate the approximate distance scale probed by the angular power spectrum at the mean depth of the sample determined from the 27 mock 2MASS catalogues. At the very smallest l -modes, the $K_s < 13.5$ power spectrum probes scales of $\gtrsim 500 h^{-1}$ Mpc.

We have also calculated the linear prediction corresponding to the Λ CDM Hubble Volume input parameters ($\Omega_m=0.3$, $\Omega_\Lambda=0.7$, $\Omega_b=0.04$, $h=0.7$, $\sigma_8=0.9$ and $\Omega_\nu=0$) through a spherical Bessel function transform of the three-dimensional power spectrum as described in section 3.2; this is indicated for a bias of 1.0 by the dashed line. The linear model and the mean mock 2MASS power spectrum are in good agreement at large scales. At smaller angular scales ($l > 30$) the effects of non-linear clustering become significant.

In order to verify whether the form and scatter of the mock power spectra, which we later use to estimate the error on the observed angular power spectrum, is consistent with the data, we perform a χ^2 fit between the two. We marginalise over the normalisation of the mean mock angular power spectrum and use the binning as shown in order to reduce the covariance to insignificant levels. We assume that the spread in the mock power spectra is independent of normalisation, i.e. we apply the same spread determined for the unbiased mock power spectra to the observed angular power spectrum. In this particular case, this is likely to provide an optimistic view of the observed errors since we are not shot noise limited. In this scenario, the errors are likely to be independent of the power spectrum amplitude; on the other hand, if the observed power spectrum

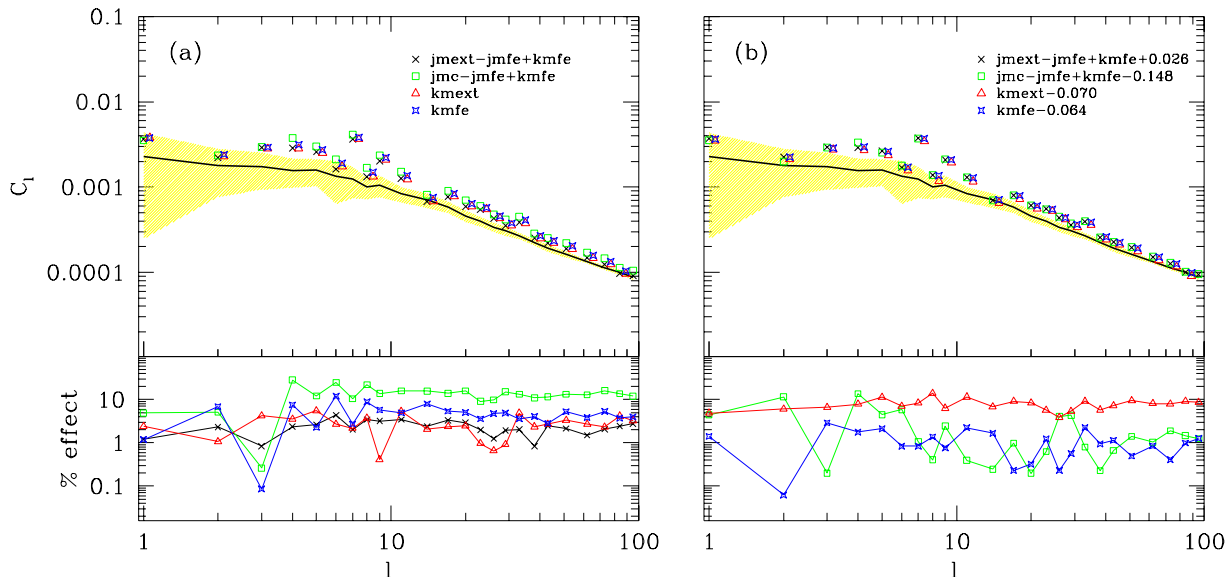


Figure 3. The $|b| > 20^\circ$, $K_s < 13.5$ extinction-corrected 2MASS galaxy angular power spectra for the four magnitude estimators shown in Fig. 1 using (a) the raw magnitude estimate and (b) a zero-point correction to account for the offset determined with respect to the Loveday (2000) photometry. The 1σ spread and mean 2MASS mock power spectrum are shown as in Fig. 2. The lower panels indicate the effect of each magnitude estimator on the resulting power spectrum compared to the colour-corrected J -band extrapolated magnitude estimator (with the zero-point correction) used in Fig. 2 and also indicated here by the black crosses in panel (b). In the upper panels we have displaced the kmext and kmfe datapoints for clarity.

is cosmic variance limited the errors scale with model normalisation (see Feldman, Kaiser & Peacock (1994) for further discussion on this point). We investigate the impact of this assumption on the associated cosmological constraints in section 5. First, we perform a χ^2 fit over the full angular range $1 \leq l \leq 100$ between the $K_s < 13.5$ 2MASS galaxy angular power spectrum and the mean mock 2MASS power spectrum; we find that $\chi^2/d.o.f.=3.0$. Limiting the angular range to scales which are not significantly affected by non-linear clustering ($l \geq 30$), the form of the mock power spectra are in better agreement with the observed 2MASS galaxy angular power spectrum, with $\chi^2/d.o.f.=2.0$.

The form of the 2MASS angular power spectrum is therefore in good agreement with the Λ CDM prediction in the linear regime, although it is clear from Fig. 2a that there is some difference in slope at small scales. Assuming the validity of the prediction, this is due either to scale-dependent bias in the non-linear regime or resolution effects in the Hubble Volume simulation. Consistency with the Λ CDM prediction in the linear regime, of interest in this work, is confirmed through a comparison (in the lower panel) with the linear prediction for the Λ CDM Hubble Volume simulation input parameters applying a scale-independent bias to match the normalisation of the observed power spectrum at large scales (see section 5).

4 SYSTEMATIC ERRORS

4.1 Magnitude Limits

Before turning to the cosmological constraints inferred from the 2MASS galaxy angular power spectrum it is important to verify that the results are robust and not significantly affected by potential sources of systematic error. While the 2MASS catalogue is >98 per cent reliable for $|b| > 20^\circ$, $K_s < 13.5$ galaxies (Jarrett et al. 2000) and 99 per cent complete for $|b| > 30^\circ$, $12.0 < K_s < 13.7$ galaxies (Maller et al. 2005), we wish to verify that the angular power spectrum is robust to changes in the magnitude limit, and is not adversely affected by variable incompleteness or reliability at faint magnitudes or scale errors in the photometry.

Fig. 2 shows the 2MASS galaxy angular power spectrum as a function of imposed magnitude limit. The shape and normalisation of the power spectrum, with respect to both the linear model and the mean mock 2MASS power spectrum, are remarkably robust to changes in the magnitude limit. The departure of the linear model from the observed power spectrum occurs at larger angular scales with the shallower magnitude limit due to the reduced mean depth of the sample. For this reason also, the mock 2MASS power spectrum is more significantly distorted at the very smallest scales by resolution effects resulting in a slightly steeper slope at $l \gtrsim 70$.

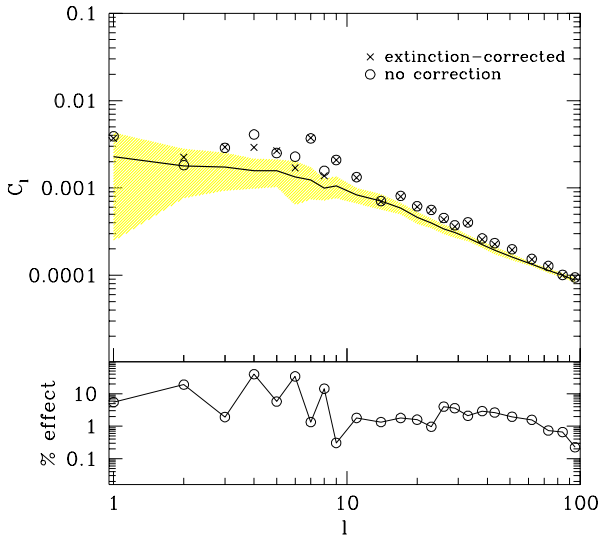


Figure 4. The $|b| > 20^\circ$, $K_s < 13.5$ 2MASS galaxy angular power spectra including no extinction correction, and as previously an extinction correction derived from the Schlegel et al. (1998) dust maps. The mock 2MASS mean angular power spectrum and 1σ spread are shown as before. In the lower panel we indicate the effect of this correction on the power spectrum through a comparison with the corrected sample (indicated by the crosses in the upper panel and as shown in Fig 2a).

4.2 Magnitude Estimator

Throughout this paper, we estimate the K_s -band magnitudes using the J -band extrapolated magnitudes colour-corrected using the K_s and J -band fiducial elliptical Kron magnitudes, as this results in a smaller zero-point offset and scale error when compared to the more accurate K -band photometry of Loveday (2000). We wish to investigate the effect on the power spectrum by the choice of magnitude estimator; in Fig. 3a and b we compare the power spectra for the four magnitude estimators presented in Fig. 1 with and without respectively the associated correction to the Loveday (2000) zero-point.

The power spectrum is robust to changes in the magnitude estimate and zero-point at the $\lesssim 10$ per cent level. This is due to the fact that the change in the depth of the survey due to differences in the magnitude limit and scale error effects are insignificant.

4.3 Extinction

While the level of extinction in the K_s -band is low and the 2MASS magnitudes have been corrected using the Schlegel et al. (1998) dust maps, it is useful to examine the potential level of systematic error introduced by extinction. Fig. 4 shows the 2MASS galaxy angular power spectrum with and without correction for extinction. In this extreme case, the effect of removing the dust correction to the mag-

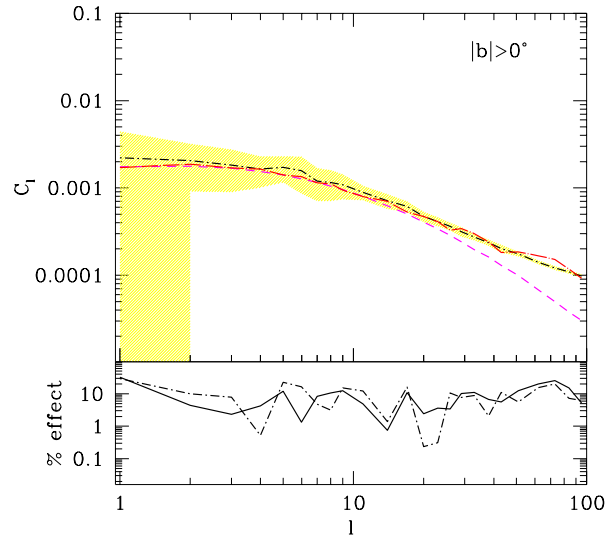


Figure 5. The $|b| > 0^\circ$, $K_s < 13.5$ mean power spectrum and 1σ spread determined from the 27 mock 2MASS catalogues (solid line and shaded region). As in Fig. 2a the dashed line indicates the expected linear trend for the Λ CDM Hubble Volume mock input parameters of $\Omega_m=0.3$, $\Omega_b=0.04$, $h=0.7$ and $\sigma_8=0.9$. As a consistency check, we also show the Λ CDM Hubble Volume non-linear power spectrum (large dot-dashed line) calculated via the numerically-determined Λ CDM Hubble Volume $P(k)$ (Carlton Baugh - priv. comm.) transformed to the angular power spectrum as described in section 3.2. In the lower panel we compare this prediction with the $|b| > 0^\circ$ (dot-dashed line) and $|b| > 20^\circ$ (solid line) mean mock 2MASS power spectra.

nitude estimate is at the $\lesssim 10$ per cent level at large scales and $\lesssim 1$ per cent above $l \approx 10$.

4.4 The Window Function

Throughout this paper a $|b| > 20^\circ$ galactic latitude cut is applied in order to avoid the high levels of extinction and stellar contamination in the zone of avoidance. We wish to determine the level of any systematic effect on the spread of the Hubble Volume mock power spectra (and therefore our interpretation of the statistical uncertainty) introduced by the window function. In Fig. 5 the 27 mock 2MASS power spectra and corresponding linear theory model for the Λ CDM Hubble Volume input parameters are shown with no galactic latitude cut. Neither the shape nor the spread of the power spectra are significantly altered. The effect of the window function on the angular power spectrum is $\lesssim 5$ per cent at all scales.

In order to check the consistency of our results we provide a further verification of the mock 2MASS power spectrum results through a comparison with the transform of the numerically-determined Λ CDM Hubble Volume simulation $P(k)$ (Carlton Baugh - priv. comm.). There is good agree-

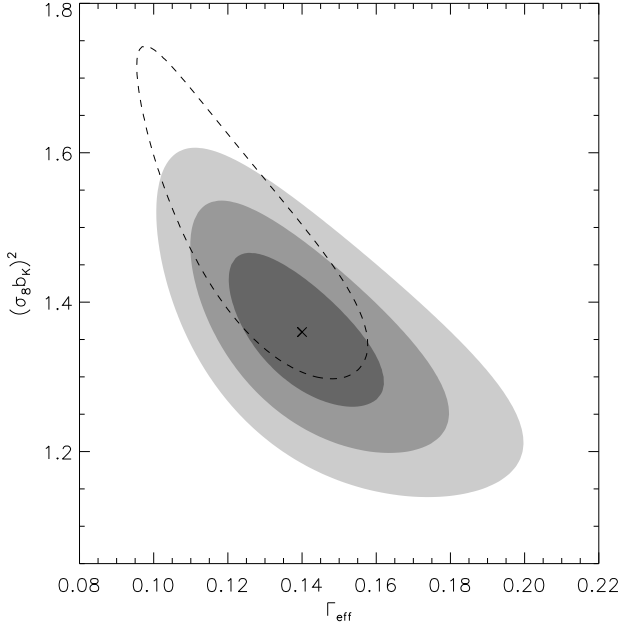


Figure 6. Filled contours representing the 1σ , 2σ and 3σ confidence regions for the galaxy power spectrum shape and normalisation determined from χ^2 fits to the 2MASS $|b| > 20^\circ$ $K_s < 13.5$ galaxy angular power spectrum in the range $l \leq 30$. The cross indicates the best fit parameters of $\Gamma_{eff} = 0.14$ and $(\sigma_8 b_K)^2 = 1.36$. We also show the 1σ confidence region for the 2MASS result as above where we use errors which scale with the model power spectrum normalisation (dashed line).

ment with both the $|b| > 0^\circ$ and $|b| > 20^\circ$ mean mock 2MASS power spectra.

5 COSMOLOGICAL CONSTRAINTS

Using the 2MASS galaxy angular power spectrum we have determined the form of the galaxy density field at extremely large scales and verified that it is not significantly affected by common sources of systematic error. We now wish to determine the associated cosmological constraints.

Using the Eisenstein & Hu (1998) transfer function fitting formulae we have determined linear theory predictions for the three-dimensional power spectrum of matter, $P(k)$, using input parameters of Ω_m , Ω_Λ , Ω_b , h and matter power spectrum normalisation, σ_8 ; in the subsequent analysis we assume a negligible neutrino mass density, a primordial $n_s = 1$ spectrum and $\Omega_\Lambda = 1 - \Omega_m$. We form galaxy angular power spectrum predictions using the spherical Bessel function transform described in section 3.2 and a linear biasing scheme.

First, we perform fits to the galaxy power spectrum shape and normalisation. Assuming a CDM cosmology, the power spectrum can be defined through a parameterisation of the shape

$$\Gamma_{eff} = \Omega_m h \exp(-\Omega_b(1 + \sqrt{2h/\Omega_m})) \quad (7)$$

(Sugiyama 1995), and a normalisation, which for galaxy

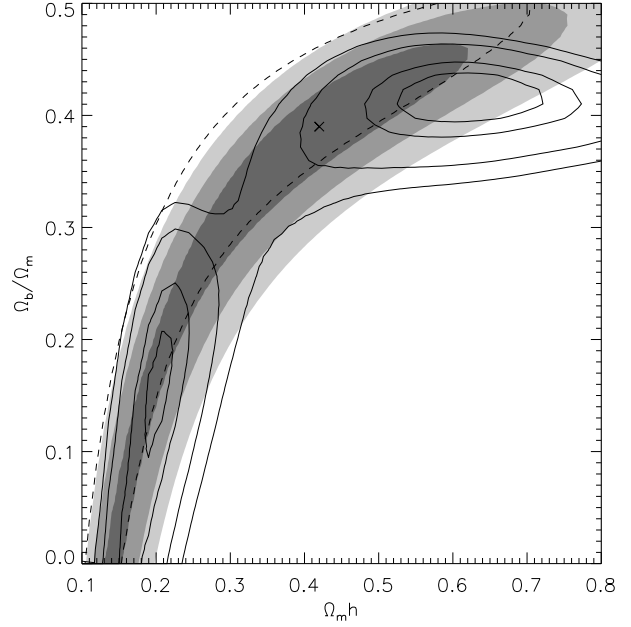


Figure 7. Contours of decreasing likelihood in the $\Omega_m h - \Omega_b/\Omega_m$ plane for the best-fitting angular power spectrum in the range $l \leq 30$. The filled contours indicate the 1σ , 2σ and 3σ confidence regions for the 2MASS $|b| > 20^\circ$ $K_s < 13.5$ galaxy angular power spectrum, determined from simple χ^2 fits, marginalising over the normalisation and h . The solid contours indicate the 1σ , 2σ , 3σ and 4σ confidence regions determined from the 2dFGRS 100k release $P(k)$ (Percival et al. 2001). The cross marks the best fit model to the 2MASS data of $\Omega_m h = 0.42$ and $\Omega_b/\Omega_m = 0.39$. As in Fig. 6 we also show the 1σ confidence region for the 2MASS result as above where we use errors which scale with the model power spectrum normalisation (dashed line).

power spectra may be parameterised through the galaxy bias and σ_8 . We constrain Γ_{eff} and $(\sigma_8 b_K)^2$ using a grid of 200×800 models between $0.1 \leq \Gamma_{eff} \leq 0.3$ and $0.0 \leq (\sigma_8 b_K)^2 \leq 8.0$ respectively. We perform least squares fits to the $|b| > 20^\circ$, $K_s < 13.5$ angular power spectrum as shown in Fig. 2a at scales of $l \leq 30$ (binned as shown to reduce the covariance to insignificant levels); beyond $l \approx 30$ the angular power spectrum begins to be significantly affected by non-linear effects.

We take the spread determined from the 27 mock 2MASS angular power spectra in order to estimate the errors on the 2MASS datapoints, assuming that the uncertainty remains the same for a biased as for an unbiased distribution (as in section 3.3). In doing this, we assume that the Λ CDM Hubble Volume mock catalogue provides an accurate description of the local galaxy distribution at large scales and that the associated uncertainty in the datapoints is realistic. However, since these errors are valid only in an unbiased Λ CDM cosmology we are required to make assumptions as to the nature of the cosmic variance in the various other cosmologies scrutinised in these fits. Here we assume that the errors are independent of cosmology and power spectrum normalisation; the likely impact of this assumption is examined below. We find that:

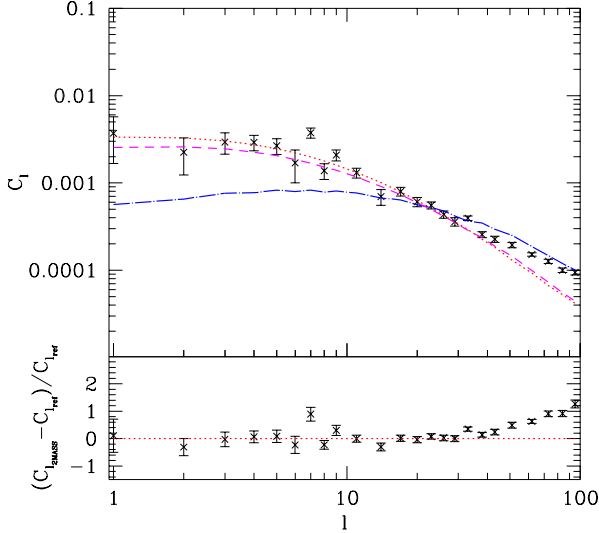


Figure 8. The angular power spectrum for $|b| > 20^\circ$ $K_s < 13.5$ 2MASS galaxies (as in Fig. 2a) is compared to a linear theory Λ CDM prediction using input parameters of $\Omega_m=1.0$, $\Omega_b=0.04$, $h=0.50$ (dot-dashed line), a Λ CDM prediction using the Hubble Volume input parameters as before (dashed line), and the best fit power spectrum shape (for $l \leq 30$) of $\Gamma_{eff}=0.14$ (dotted line). In each case we use the best fit normalisation of $(\sigma_8 b_K)^2 = 1.36$. The errorbars indicate the 1σ spread determined from the 27 mock 2MASS power spectra. In the lower panel we show the fractional deviation from the best fit $\Gamma_{eff}=0.14$ prediction.

$$\Gamma_{eff} = 0.14 \pm 0.02$$

and

$$(\sigma_8 b_K)^2 = 1.36 \pm 0.10$$

marginalising over the normalisation and power spectrum shape respectively. The associated confidence regions are indicated by the filled contours in Fig. 6.

This value of Γ_{eff} is in excellent agreement with the 2dFGRS fit (Percival et al. 2001) of $\Gamma_{eff} = 0.18 \pm 0.04$ (for $h=0.7$) and the WMAP value (Spergel et al. 2003) of $\Gamma_{eff} = 0.15 \pm 0.01$ (for $n_s=0.99$). However, our value is slightly higher than the Maller et al. (2005) result which constrains $\Gamma_{eff} = 0.116 \pm 0.009$ at 95 per cent confidence using a measure of the three-dimensional K_s -band galaxy power spectrum via an inversion of the 2MASS angular correlation function.

Our constraint on the K_s -band galaxy power spectrum normalisation of $(\sigma_8 b_K)^2 = 1.36 \pm 0.10$ is also slightly higher than the Maller et al. (2005) result of $\sigma_8 b_K = 1.0 \pm 0.1$. Using the WMAP-2dFGRS best fit matter power spectrum normalisation of $\sigma_8 = 0.84 \pm 0.04$ (Bennett et al. 2003), we constrain the K_s -band bias to $b_K = 1.39 \pm 0.12$, in reasonable agreement with previous measurements determined from the

2MASS clustering dipole of $b_K = 1.37 \pm 0.34$ (Maller et al. 2003) and the 2MASS angular correlation function analysis of $b_K = 1.1 \pm 0.1$ (Maller et al. 2005). The constraint on the bias derived in this work rejects $b_K = 1$ at $> 3\sigma$; it appears therefore that galaxies selected in the K_s -band are clustered more strongly than both the underlying mass distribution and galaxies selected in optical wavebands for which $b \approx 1$ (e.g. Verde et al. 2002; Gaztañaga 1994).

We are also able to provide constraints on other cosmological parameters. We fit to $\Omega_m h$ and Ω_b/Ω_m since these primarily determine the shape of the input $P(k)$ and the size of the baryon oscillations. We determine model angular power spectra in a $71 \times 51 \times 11$ grid between $0.1 \leq \Omega_m h \leq 0.9$, $0.0 \leq \Omega_b/\Omega_m \leq 0.5$ and $0.4 \leq h \leq 0.9$ (the effect of h on the angular power spectrum is fairly small and we therefore use a lower resolution). We perform least squares fits to the $K_s < 13.5$, $|b| > 20^\circ$ angular power spectrum at scales of $l \leq 30$, using errors determined for the 2MASS datapoints as before which are independent of power spectrum normalisation.

The filled contours in Fig. 7 show the associated confidence regions marginalising over the normalisation. We are able to provide weak constraints on the cosmology of $\Omega_m h < 0.62$ and $\Omega_b/\Omega_m < 0.46$ (at 1σ confidence). These constraints are particularly insensitive to the baryon density since the acoustic oscillations detected in redshift survey analyses are smoothed over a wide range of angular scales. However our constraints are in good agreement with the previous results at smaller scales from the 2dFGRS $P(k)$ (Percival et al. 2001; Cole et al. 2005). As an example of how our results can differentiate between different cosmological models we show the 2MASS galaxy angular power spectrum compared with Λ CDM and SCDM predictions in Fig. 8.

We also wish to examine our assumption, used throughout this work, that the uncertainty due to cosmic variance determined from the 27 Λ CDM mock 2MASS catalogues is independent of the power spectrum normalisation. To do this, we instead assume that the errors determined from the Λ CDM mock catalogues simply scale with the model power spectrum normalisation as would be the case in the cosmic variance limited scenario, and compare the two cases. In Figs. 6 and 7 we show the associated 1σ confidence regions by the dashed lines, marginalising over the power spectrum normalisation. We find best fit parameters of $\Gamma_{eff}=0.125 \pm 0.030$, $(\sigma_8 b_K)^2 = 1.47^{+0.27}_{-0.17}$, $\Omega_b/\Omega_m < 0.52$ and $\Omega_m h < 0.71$. This constraint on the galaxy power spectrum normalisation implies a K_s -band bias of $b_K = 1.44^{+0.21}_{-0.14}$ (using the WMAP-2dFGRS constraint on σ_8 as before). It is clear that while the associated confidence regions for each parameter are slightly larger the results are in fair agreement whichever error analysis is used. However, it is clear from Fig. 6 that using this alternative assumption about the errors it is more difficult to reject combinations of high bias and steeper Γ_{eff} slopes. For example, $\Gamma_{eff}=0.05$ would only be rejected at 2.5σ . More simulations of other cosmologies are needed to check whether these errors or the errors used elsewhere in this paper are most likely to be correct.

6 CONCLUSIONS

We have used 518 576 $K_s < 13.5$, $|b| > 20^\circ$ galaxies selected from the 2MASS full release extended source catalogue to determine the associated angular power spectrum and constrain the form of galaxy fluctuations to Gigaparsec scales. We have compared this to a Λ CDM N-body mock prediction constructed from the Hubble Volume simulation; it is in reasonable agreement although there is a discrepancy in the slopes at $l > 30$ in that the 2MASS result is significantly steeper than the mock prediction. We compare these to a linear theory prediction using the Λ CDM Hubble Volume simulation input parameters; there is good agreement with the mock prediction at scales where non-linear effects are insignificant ($l \lesssim 30$).

Possible sources of systematic error were investigated. We first examined the effect of imposed magnitude limit; the 2MASS angular power spectrum slope was robust with respect to the 2MASS mock and model predictions. The 2MASS galaxy angular power spectrum is also robust to different magnitude estimators and zero-point corrections (imposed to agree with the Loveday (2000) photometry) at the ≈ 10 per cent level. We correct for extinction using the Schlegel et al. (1998) dust maps; the effect on the angular power spectrum is ≈ 10 per cent at $l \lesssim 10$, and ≈ 1 per cent at smaller scales. Our results are also robust to window function effects; the effect of a $|b| > 20^\circ$ cut is $\lesssim 5$ per cent at all scales.

Finally, we have used linear theory predictions for the 2MASS galaxy angular power spectrum formed from the transfer function fitting formulae of Eisenstein & Hu (1998) to determine constraints on $\Omega_m h$ and Ω_b/Ω_m assuming a flat CDM cosmology, a primordial $n_s=1$ spectrum and a negligible neutrino mass. Our results are in agreement with the 2dFGRS $P(k)$ constraints (Percival et al. 2001), and we are able to provide weak constraints of $\Omega_m h < 0.62$ and $\Omega_b/\Omega_m < 0.46$ (at 1σ confidence). Angular power spectrum analysis is particularly insensitive to the baryon density since any associated baryon oscillations are likely to be smoothed over a wide range of angular scales. However, given the huge volume probed (≈ 5 times the final 2dFGRS volume) the associated constraints on the power spectrum shape and normalisation are more significant. We also determine constraints for the galaxy power spectrum shape, Γ_{eff} , and normalisation, $(\sigma_8 b_K)^2$. In agreement with the 2dFGRS and WMAP values, we find that $\Gamma_{eff} = 0.14 \pm 0.02$. This is slightly higher than an alternative value found by Maller et al. (2005) using the 2MASS dataset of $\Gamma_{eff} = 0.116 \pm 0.009$, determined through an inversion of the angular correlation function. We also tightly constrain the K_s -band galaxy power spectrum normalisation to $(\sigma_8 b_K)^2 = 1.36 \pm 0.10$. Using the WMAP-2dFGRS value of $\sigma_8 = 0.84 \pm 0.04$ (Bennett et al. 2003), this implies a K_s -band bias of $b_K = 1.39 \pm 0.12$.

We also investigated the likely impact on our assumption that the errors which we use to constrain various cosmological parameters, determined from the unbiased Λ CDM mocks, are independent of cosmology and power spectrum normalisation by instead assuming that these errors simply scale with the power spectrum normalisation as would be the case in the cosmic variance limited scenario. We find that while the associated confidence regions are slightly larger

the results are in fair agreement. However it becomes less easy to reject models with lower Γ_{eff} ; therefore although the data appears to prefer a Λ CDM power spectrum slope, it may still not be possible to rule out a significantly steeper Γ_{eff} .

ACKNOWLEDGEMENTS

This publication makes use of data products from the 2 Micron All-Sky Survey, which is a joint project of the University of Massachusetts and the Infrared Processing and Analysis Centre/California Institute of Technology, funded by the Aeronautics and Space Administration and the National Science Foundation. We thank Shaun Cole for useful discussion, Tom Jarrett for his help with the 2MASS magnitudes, Adrian Jenkins and Carlton Baugh for their assistance with the Hubble Volume mock catalogues, and Will Percival for providing the 2dFGRS constraints. We also thank David Johnston for useful comments.

REFERENCES

- Baugh, C.M. & Efstathiou, G. 1993, MNRAS, 265, 145
- Bennett, C.L. et al. 2003, ApJS, 148, 1
- Bruzual, A.G., & Charlot, S. 1993, ApJ, 405, 538
- Buswell, G.S., Shanks, T., Outram, P.J., Frith, W.J., Metcalfe, N. & Fong, R. 2004, MNRAS, 354, 991
- Cole, S.M. et al. 2001, MNRAS, 326, 555
- Cole, S.M. et al. 2005, submitted to MNRAS, astro-ph/0501174
- Colless, S. et al. 2001, astro-ph/0306581
- Driver, S. 2003, IAUS, 216, 97
- Eisenstein, D.J. & Hu, W. 1998, ApJ, 496, 605
- Feldman, H.A., Kaiser, N. & Peacock, J.A. 1994, ApJ, 426, 23
- Frith, W.J., Buswell, G.S., Fong, R., Metcalfe, N. & Shanks, T. 2003, MNRAS, 345, 1049
- Frith, W.J., Shanks, T. & Outram, P.J. 2004, astro-ph/0408011
- Frith, W.J., Shanks, T. & Outram, P.J. 2005, submitted to MNRAS, astro-ph/0411204
- Gaztañaga, E. 1994, MNRAS, 268, 913
- Peebles, P.J.E. & Hauser, M.G. 1973, ApJ, 185, 757
- Hawkins, E. et al. 2003, MNRAS, 346, 78
- Huterer, D., Knox, L. & Nichol, R.C. 2001, ApJ, 555, 547
- Jarrett, T.H., Chester, T., Cutri, R., Schneider, S., Skrutskie, M. & Huchra, J.P. 2000, AJ, 119, 2498
- Jarrett, T.H. 2004, astro-ph/0405069
- Jenkins, A. et al. 1998, ApJ, 499, 20
- Heath, D.H. et al. 2004, MNRAS, 355, 747
- Loveday, J. 2000, MNRAS, 312, 517
- Loveday, J., Peterson, B.A., Maddox, S.J. & Efstathiou, G. 1996, ApJS, 107, 201
- Loveday, J. 2004, MNRAS, 347, 601L
- Maddox, S.J., Sutherland, W.J., Efstathiou, G. & Loveday, J. 1990, MNRAS, 243, 692
- Maller, A.H., McIntosh, D.H., Katz, N. & Weinberg, M.D. 2003, ApJ, 598, 1
- Maller, A.H., McIntosh, D.H., Katz, N. & Weinberg, M.D. 2005, ApJ, 619, 147

- Metcalf, N., Fong, R. & Shanks, T. 1995, MNRAS, 274, 769
- Metcalf, N., Shanks, T., Campos, A., McCracken, H.J. & Fong, R. 2001, MNRAS, 323, 795
- Outram, P.J., Hoyle, F., Shanks, T., Croom, S.M., Boyle, B.J., Miller, L., Smith, R.J. & Myers, A.D. 2003, MNRAS, 342, 483
- Peebles, P.J.E.. 1973, ApJ, 185, 413
- Peebles, P.J.E. & Hauser, M.G. 1974, ApJS, 28, 19
- Percival et al. 2001, MNRAS, 327, 1297
- Scharf, C., Hoffman, Y., Lahav, O. & Lynden-Bell, D. 1992, MNRAS, 256, 229
- Schlegel, D.J., Finkbeiner, D.P. & Davis, M. 1998, ApJ, 500, 525
- Spergel, D.N. et al. 2003, ApJS, 148, 175
- Sugiyama, N. 1995, ApJS, 100, 281
- Tegmark, M. et al. 2002, ApJ, 571, 191
- Verde, L. et al. 2002, MNRAS, 335, 432
- Yasuda, N. et al. 2001, AJ, 122, 1104
- Zehavi, I. et al. 2002, ApJ, 571, 172